Computerized Medical Imaging and Graphics 33 (2009) 171–181

Contents lists available at ScienceDirect

Computerized Medical Imaging and Graphics

journal homepage: www.elsevier.com/locate/compmedimag

Assessment of 3D DCE-MRI of the kidneys using non-rigid image registration and segmentation of voxel time courses

Frank G. Zöllner[a,b,*], Rosario Sance[e], Peter Rogelj[f], María J. Ledesma-Carbayo[e], Jarle Rørvik[a,c], Andrés Santos[e], Arvid Lundervold[c,d]

[a] Section for Radiology, Department of Surgical Sciences, University of Bergen, N-5021 Bergen, Norway
[b] Computer Assisted Clinical Medicine, Faculty of Medicine Mannheim, University of Heidelberg, Theodor-Kutzer-Ufer 1-3, D-68167 Mannheim, Germany
[c] Department of Radiology, Haukeland University Hospital, Bergen, Norway
[d] Section for Physiology, Department of Biomedicine, University of Bergen, Jonas Lies vei 91, N-5009 Bergen, Norway
[e] Biomedical Image Technologies, Universidad Politécnica de Madrid, E.T.S.I. Telecomunicación, E-28040 Madrid, Spain
[f] Faculty of Electrical Engineering, University of Ljubljana, Trzaska 25, SI-1000 Ljubljana, Slovenia

ARTICLE INFO

Article history:
Received 24 May 2007
Received in revised form 10 October 2008
Accepted 21 November 2008

Keywords:
DCE-MRI
Kidney
Multi-modality non-rigid image registration
k-means clustering
Time series analysis
Renal function

ABSTRACT

We have applied automated image analysis methods in the assessment of human kidney perfusion based on 3D dynamic contrast-enhanced MRI data. This approach consists of non-rigid 3D image registration of the moving kidney followed by *k*-means clustering of the voxel time courses with split between left and right kidney. This method was applied to four data sets acquired from healthy volunteers, using 1.5 T (2 exams) and 3 T scanners (2 exams).

The proposed registration method reduced motion artifacts in the image time series and improved further analysis of the DCE-MRI data. The subsequent clustering to segment the kidney compartments was in agreement with manually delineations (similarity score of 0.96) in the same motion corrected images. The resulting mean intensity time curves clearly show the successive transition of contrast agent through kidney compartments (cortex, medulla, and pelvis). The proposed method for motion correction and kidney compartment segmentation might improve the validity and usefulness of further model-based pharmacokinetic analysis of kidney function in patients.

1. Introduction

The kidneys maintain normal homeostasis by filtering and excreting metabolic waste products, by regulating acid–base balance, and by moderating blood pressure and fluid volume [1]. Decrease in renal function is caused by many disorders, among these are diabetes mellitus and hypertension. Chronic renal failure is an increasing problem world-wide; up to 5% of the world's population may in the near future suffer from end-stage renal disease (ESRD), with dialysis or kidney transplantation as the costly therapeutic alternatives [2]. Furthermore, renovascular disease seems to be an individual risk factor for cardiovascular disease [3]. Therefore, it is important – for patients and society – that methods are developed to monitor renal function precisely, thus enhancing the assessment of disease progression, the prognosis, and follow-up therapy.

At present, diagnosis of renal dysfunction is based on such measurements as creatinine, urea, and electrolytes, as well as on creatinine clearance. These indirect measurements have low sensitivity, since a significant change in creatinine level is only detectable after a 60% function loss has occurred, while creatinine clearance overestimates the actual glomerular filtration rate (GFR) by up to 20% [4]. In addition, these clinical chemistry measurements cannot detect local differences in the kidneys and cannot distinguish between left and right kidney. To overcome these limitations, dynamic contrast-enhanced MR imaging (DCE-MRI) has emerged as a technique that can be used for the more accurate assessment of regional renal function [5,6]. With this technique, signal intensity evolution can be measured and visualized as images that reflect the passage of an injected tracer or contrast agent through the organ.

An important obstacle to these dynamic measurement techniques that complicates further analysis is the *movement* of the organ of interest during image acquisitions, when the individual voxels undergo complex displacements due to respiratory motion and pulsation. Such movements are often overlooked in studies of renal function [7–9]. However, without proper *motion correction*,

* Corresponding author at: Computer Assisted Clinical Medicine, Faculty of Medicine Mannheim, University of Heidelberg, Theodor-Kutzer-Ufer 1-3, D-68167 Mannheim, Germany. Tel.: +49 621 383 5117; fax: +49 621 383 5123.
E-mail addresses: frank.zoellner@medma.uni-heidelberg.de (F.G. Zöllner), rsance@die.upm.es (R. Sance), peter.rogelj@fe.uni-lj.si (P. Rogelj), mledesma@die.upm.es (M.J. Ledesma-Carbayo), jarr@haukeland.no (J. Rørvik), andres@die.upm.es (A. Santos), arvid.lundervold@biomed.uib.no (A. Lundervold).

0895-6111/$ – see front matter © 2008 Elsevier Ltd. All rights reserved.
doi:10.1016/j.compmedimag.2008.11.004

the derived voxel time courses will not represent spatially fixed kidney volume elements, thus invalidating a major assumption underlying subsequent voxel-based time series analysis and pharmacokinetic modeling. A major contribution of the present work is that we performed geometric correction of these movements by introducing *multi-modality non-rigid image registration techniques*. The use of these techniques can improve the applicability and clinical value of recent developments in renal multi-compartment modeling, in simulation, and in image-based estimation of renal function [10–13].

Another important issue in analyzing kidney function using DCE-MRI is the *detection and segmentation of the renal compartments*. Accurate parenchyma sub-segmentation enables the assessment of signal intensity time curves for those regions, leading to a more comprehensive evaluation of the status of the organ and of its functional compartments [14,10].

The assessment of MRI time series is usually carried out manually or semi-automatically [6,15,16]. Typically, the user delineates a region of interest (ROI) from which a (mean) voxel time course is extracted. In this way the ROIs are generally selected based on the user's knowledge of anatomy. Valuable information inherent in the signal intensity time courses is not used. Manual ROI placements are also subject to inter- and intra-observer variability [15]. An additional disadvantage of such methods is that they are slow, even though semi-automatically techniques do reduce the processing time [17]. Automated computational techniques can overcome these drawbacks. Unsupervised data-driven approaches such as clustering of the voxel time courses may lead to more accurate and objective segmentation within reasonable time.

In this paper we present an automated 3D non-rigid image registration and pattern recognition technique, applied to dynamic contrast-enhanced MR imaging, to extract useful voxel-based functional information from the kidney.

2. Related work

2.1. Image registration

During the past three decades several registration techniques have been developed and applied to medical imaging. Comprehensive surveys are presented in [18,19]. In the present work we have focused on non-rigid (deformable) registration methods relevant in cases where the imaged object can become deformed during the observation time. A high degree of deformation and displacement is especially prominent in dynamic cardiac imaging, breast imaging, and abdominal imaging.

Motion correction of contrast-enhanced image time series is a special case of image registration, where two types of motion and deformation are present and visible in the images. The first type is motion and deformation of tissues as a result of e.g. breathing or pulsation, while the second is motion of the contrast agent. To correct for motion resulting from breathing and pulsation, the registration method needs to be unaffected by intensity changes caused by the accumulation and excretion of the contrast agent.

A solution for tissue displacement in the registration of contrast-enhanced kidney time series was proposed by Lee et al. [20]. They aligned kidneys on the basis of their centers of gravity computed from predefined contours around each individual kidney and for each time point. Another approach to the registration of kidney data sets was proposed by Sun et al. [21]. These authors posed an energy minimization method, through the integration of a subpixel motion model and temporal smoothness constraints. From experimental observations on contrast-enhanced renal perfusion MRI images of the rat kidney, they concluded that the movement introduced by breathing is mainly a head-to-feet motion with a subpixel displacement. In contrast to these methods that deal with 2D dynamic series and involve either manual intervention or head-to-feet constraints, Song et al. [22] proposed an automated 3D registration framework based on wavelet and Fourier transforms. Their algorithm consists of three steps: first, de-noising by edge-preserving anisotropic diffusion; second, edge detection by 3D dyadic wavelet expansion; and third, 3D rigid registration based on Fourier transform. Another important solution was proposed by Rohlfing et al. [23] for modeling liver motion and deformation. Their intensity-based non-rigid registration method uses B-spline deformation model and normalized mutual information as a similarity measure.

To compensate for the motion and deformation of the human kidneys during DCE-MRI acquisitions, we have used an approach similar to Rohlfing et al. [23]. We focused on multi-modality registration techniques, which enable the registration of images with complex intensity dependencies, e.g., of images acquired with different imaging techniques. In our case, these approaches provide the invariance to the presence and flow of the contrast agent. Thus, individual images of the time series can be independently registered on the selected reference frame, without using any temporal constraints. This assures that temporal information is not distorted, which is important, since temporal information is later used for the analysis of renal function.

2.2. Voxel-based time series analysis

In order to analyze voxel-based time series automatically, without the need of manual interaction for segmentation of left and right kidney and their functional compartments, we present a fully data-driven approach based on clustering. Clustering has been successfully applied in fMRI, especially for contrast-enhanced perfusion studies of the brain [24–26], DCE-MRI of the breast [27], or automatic arterial input function selection [28]. Clustering seems also to be reasonable for the analysis of the perfusion time series of the human kidney. In our approach we have applied k-means clustering [29] to split the function of left and right kidney automatically, and to obtain different regions of the kidney according to their dynamic contrast enhancement patterns.

3. Materials and methods

3.1. Data and acquisition

In the present study we have used two different pulse-sequences for the acquisition of 3D perfusion time series having a different temporal and spatial resolution as well as a different length. On the 1.5 T Siemens Symphony scanner and 3.0 T Sigma Excite GE we used a 3D volumetric interpolated breath-hold examination (VIBE) and a 3D liver acceleration volumetric acquisition (LAVA), respectively. Altogether, four data sets were obtained in four exams; each exam resulted in one data set. Table 1 gives the main acquisition parameters. All data were recorded from healthy volunteers, 1 female (exams 2 and 3) and 2 males (exams 1 and 4). The study was approved by the regional Ethical Committee of Western Norway.

Exams 1 and 2 used the VIBE protocol with flip angle = 9°, TR = 3.3 ms, and TE = 1.79 ms. Exam 3 used the LAVA protocol with flip angle = 12°, TR = 2.59 ms, TE = 1.10 ms, whereas exam 4 used this protocol with flip angle = 12°, TR = 2.74 ms, and TE = 1.14 ms. In all examinations a paramagnetic contrast agent was used (Omniscan,GE Healthcare, Oslo, Norway). A dose of 2 ml (0.5 mmol/ml Gadodiamide) of contrast agent was injected after recording the fifth 3D volume. In exam 1, additional 15 volumes were recorded at non-uniform time intervals. In exams 3 and 4 we recorded additional 55 volumes and in exam 2, 113 further volumes were recorded. The total acquisition time in exam 1 was 7 min 12 s with pauses of 62 s after volume 11, 70 s after volume number 16, and

Table 1
Description of the pulse-sequences (VIBE or LAVA) used in this study.

Exam	Scanner	Sequence	Spatial res (mm)	Matrix	Temporal res
1	1.5 T	VIBE	(1.48 × 1.48 × 3.00)	(256 × 256 × 20 × 20)	n.e.
2	1.5 T	VIBE	(1.48 × 1.48 × 3.00)	(256 × 256 × 20 × 118)	2.5 s
3	3.0 T	LAVA	(0.86 × 0.86 × 2.4)	(512 × 512 × 44 × 60)	3.0 s
4	3.0 T	LAVA	(1.72 × 1.72 × 2.4)	(256 × 256 × 22 × 60)	3.7 s

Exam 1 has been recorded with non-equidistant time sampling (n.e.).

72 s between volumes 18 and 19, respectively. The first 11 measurements were sampled at intervals of 2.5 s, the rest at 30 s per one single volume. For the other examinations, acquisitions took place for 4 min and 55 s (exam 2), 3 min (exam 3), and 3 min and 42 s for exam 4 at fixed time intervals (cf. Table 1).

3.2. Non-rigid image registration

The registration of abdominal DCE-MRI time series is a challenge. Since both rigid and non-rigid transformations are present, we chose a two-step (rigid and non-rigid) three-dimensional registration algorithm to recover these. The transformation is obtained by optimizing the similarity between the frame under investigation and a reference frame. The temporal intensity variations caused by the passage of the tracer lead us to the use of a similarity metric from statistical information theory for the whole algorithm: the Mattes implementation of the mutual information metric [30], usually chosen for multi-modality registration.

In our approach, registration starts with a simple rigid registration algorithm, where the transformation is defined by a small set of parameters and the optimization is carried out with a regular step implementation of the common gradient descent method [31]. In this way, the main head-to-feet displacement tendency can be corrected easily. The intermediate result is later used to initialize the non-rigid step.

The non-rigid transformation component incorporates an implicit spatial deformation model described by B-splines basis functions, which are uniformly placed on a grid of control points. The deformation is obtained by optimizing coefficients of these functions using a quasi-Newton BFGS optimizer [32]. A multi-resolution strategy was included in order to reduce the computational cost and to increase the robustness of the algorithm. The coarse-to-fine effect was created by sub-sampled images and by upsampling the warping grid, where the latter one served as a way of regularization. A more detailed description of the implementation can be found in [33].

Fig. 1 sketches the proposed registration method implemented in C++, using functions of the open source software toolkit *Insight Segmentation and Registration Toolkit* (ITK).

Because of the absence of standard test data, the quality of the non-rigid registration method cannot be directly assessed. Consequently, experiments are often performed on simulated data or by analyzing properties of the deformed grid or the similarity of registered images. All these methods have certain limitations. We decided to use an evaluation based on comparison with an alternative registration algorithm, which is in almost all aspects different to the algorithm described above. This alternative algorithm is based on a Gaussian deformation model, an intensity-based point similarity measure [34], and a symmetric approach [35]. The results obtained by both algorithms were compared by means of their respective intensity time courses corresponding to small regions of interest (ROIs) that were manually selected on different kidney sections. Furthermore, obtained variances within the defined ROIs were analyzed by the *F*-test [36] to investigate whether there are significant differences between the registered and unregistered data. The null hypothesis H_0: $\sigma^2_{\text{registered}} \geq \sigma^2_{\text{unregistered}}$ was tested against the alternative H_1: $\sigma^2_{\text{registered}} < \sigma^2_{\text{unregistered}}$. A significance level of 5% was set for rejecting the null hypothesis.

3.3. Voxel-based time series analysis by k-means clustering

K-means clustering [29] is an iterative process aiming at to minimize the objective function

$$E = \sum_{k=1}^{K} \sum_{x \in C_k} d(\vec{x}, \vec{m}_k) \tag{1}$$

across all clusters $C_1, \ldots, C_K$, where K is the number of predefined clusters, m_k is the centroid of cluster C_k, and $\vec{x}$ are the data points. In this approach the DCE-MRI data are represented for each voxel i as an intensity vector $\vec{I}_i = (I_i^1, \ldots, I_i^t, \ldots, I_i^T) \in \mathbb{R}^T$ where $t = 1, \ldots, T$ denotes a time point in the sequence of volume acquisitions. We found that the cosine distance function [37] was a good choice for the metric (d), i.e.

$$d(\vec{I}_i, \vec{I}_j) = 1 - \cos\alpha \tag{2}$$

where

$$\cos\alpha = \frac{\vec{I}_i \vec{I}_j}{|\vec{I}_i||\vec{I}_j|} \tag{3}$$

describes the cosine of the angle between $\vec{I}_i$ and $\vec{I}_j$ in $\mathbb{R}^T$.

Our clustering approach is depicted in Fig. 2. First, we preprocess the data by a *k*-means clustering procedure to extract automatically the single kidneys from the recorded image series, in order to provide a separation between left and right kidney. We initialized the algorithm with $K = 3$ ("cortex", "medulla", and "background"). The cluster centroid were initially chosen by random. The clustering itself was repeated ten times to not get biased due to the initialization. We performed the clustering only for the middle slice of the acquired 3D volumes and used only a short part of the sequence that

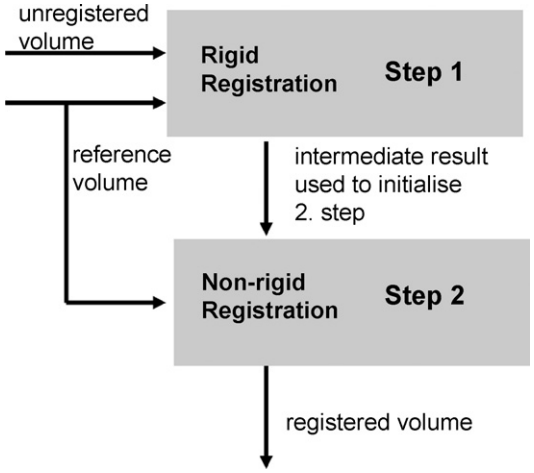

Fig. 1. Processing scheme describing our registration algorithm. The result from the first step (rigid registration) is used to initialize the second step (non-rigid registration).

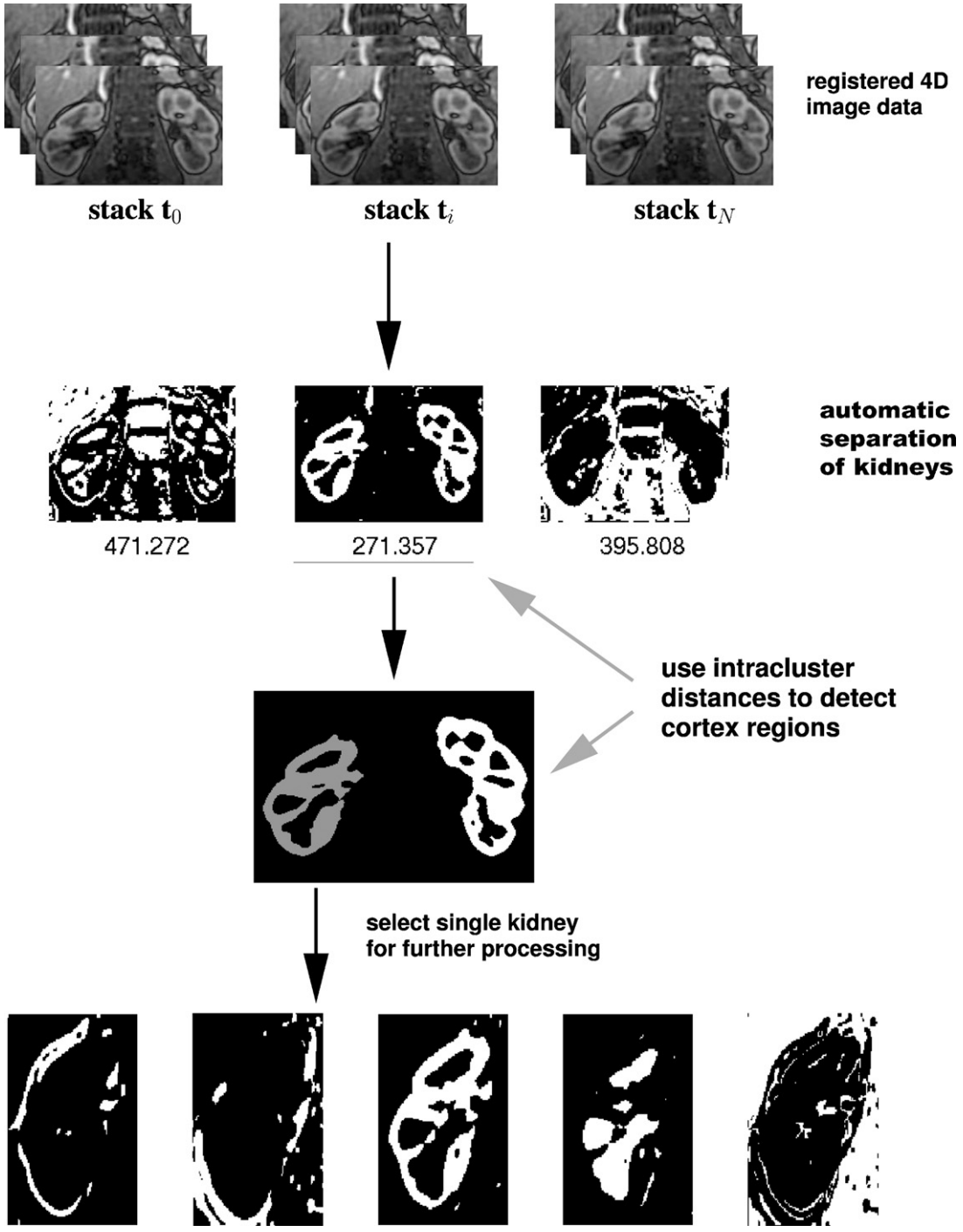

Fig. 2. Scheme for automatic clustering of motion-corrected DCE-MRI voxel time series. *K*-means ($K = 3$) clustering was first applied to detect the renal cortex and to separate the kidneys. Voxel time courses within each of the kidney masks are then clustered again. Data shown are from exam 3.

captured the initial cortical phase of the enhancement (cf. upper part of Fig. 2). The rationale behind this is twofold: firstly, assuming that the kidney is usually centered in the 3D volume, its largest extension is around the middle slice, so that a well-fitting bounding box/mask including the whole kidney is assured. Secondly, such short sequences are sufficient because the characteristic wash-in part of the intensity curve for the renal cortex is at about 15–20 s (in a healthy patient) after injection. Using this technique, the cortex could be identified easily and clearly. Moreover, the clustering of the kidney perfusion time series revealed that the cortex of the kidney can be automatically identified by the intra-cluster distance of the corresponding cluster being the minimum of all found classes. The found members of the cluster could be mapped back into an image. The separation of the kidneys is then obtained by applying connected-components-labeling and morphological operators on this image to derive a bounding box/mask.

In the second step (cf. lower part of Fig. 2), the obtained masks of each kidney are used to extract VOIs (volumes of interest) of the single kidneys from the original data. The clustering is then repeated on these voxel time series to analyze the perfusion of the renal organ. The *k*-means algorithm is initialized by 5–7 classes in order to detect and segment different compartments of the kidney. Here, similar to the initial step, random initialization of the cluster centroids was performed.

Table 2
Evaluation of uncorrected and motion-corrected DCE-MRI data with respect to signal variation within manually delineated ROIs during time.

	Exam	Data set 3			Data set 1		
	ROI	Cortex	Medulla	Pelvis	Cortex	Medulla	Pelvis
Unregistered	Mean	16.77	7.77	27.08	3.52	3.76	5.10
	Median	10.31	6.51	27.16	3.30	3.30	4.68
Proposed method	Mean	10.24	4.70	18.90	4.95	2.13	3.64
	Median	7.26	4.10	15.31	4.14	2.07	3.57
Alternative method	Mean	8.37	6.52	25.26	2.36	1.84	3.46
	Median	6.83	6.23	23.73	2.36	1.86	3.48

For each manually delineated ROI and each frame, the signal intensity standard deviation (SD) was calculated. The tabulated figures are given as mean and median of these SD values across all time-frames.

Similar to registration, the evaluation of segmentation results is difficult due to the lack of clear standards [38]. In our case we compared the automatic segmentation to manual delineated (by trained experts) regions in order to quantify the segmentation error. Commonly, overlap measures such as Dice, Jaccard/Tanimoto (TN), and Volume Similarity are applied [39]. Dice and Tanimoto (alternatively known as Jaccard Similarity) are related [38]. Volume Similarity depends only on the number of voxels in the labeled regions that are compared. It does not take the spatial relation of the labeled regions into account. Therefore, TN has been selected. TN can be defined as follows: let I_1, I_2 denote two binary images defined on a grid G of N pixels x. Let $X = \{x \in L | I_1(x) = 1\}$ be the segmented region and $Y = \{x \in L | I_2(x) = 1\}$ the manually delineated mask, then:

$$\mathrm{TN}(I_1, I_2) = \frac{|X \cap Y| + \overline{|X \cup Y|}}{|X \cup Y| + \overline{|X \cap Y|}} \tag{4}$$

TN tends towards 1 if the similarity between the sets X and Y is high.

4. Results

In this section the results of the proposed algorithms obtained for the four data sets (cf. Section 3.1 and Table 1) are presented. The overall assessment of the proposed method consists of three steps: (i) assessment of the registration method, (ii) analysis of the impact of registration to clustering, and (iii) assessment of k-means based segmentation compared to manual segmentation.

4.1. Non-rigid image registration

As outlined in Section 3.2, we compared two independent registration algorithms to assess the quality of the motion correction results. The actual comparison was made with respect to mean signal intensity time courses within fixed ROIs obtained with each registration algorithm.

Fig. 3 shows the extracted signal intensity time courses for the manually delineated ROIs, superimposed on the slices depicted on the left, belonging to each of the main kidney compartments in exams 3. As previously mentioned, the intensity time courses

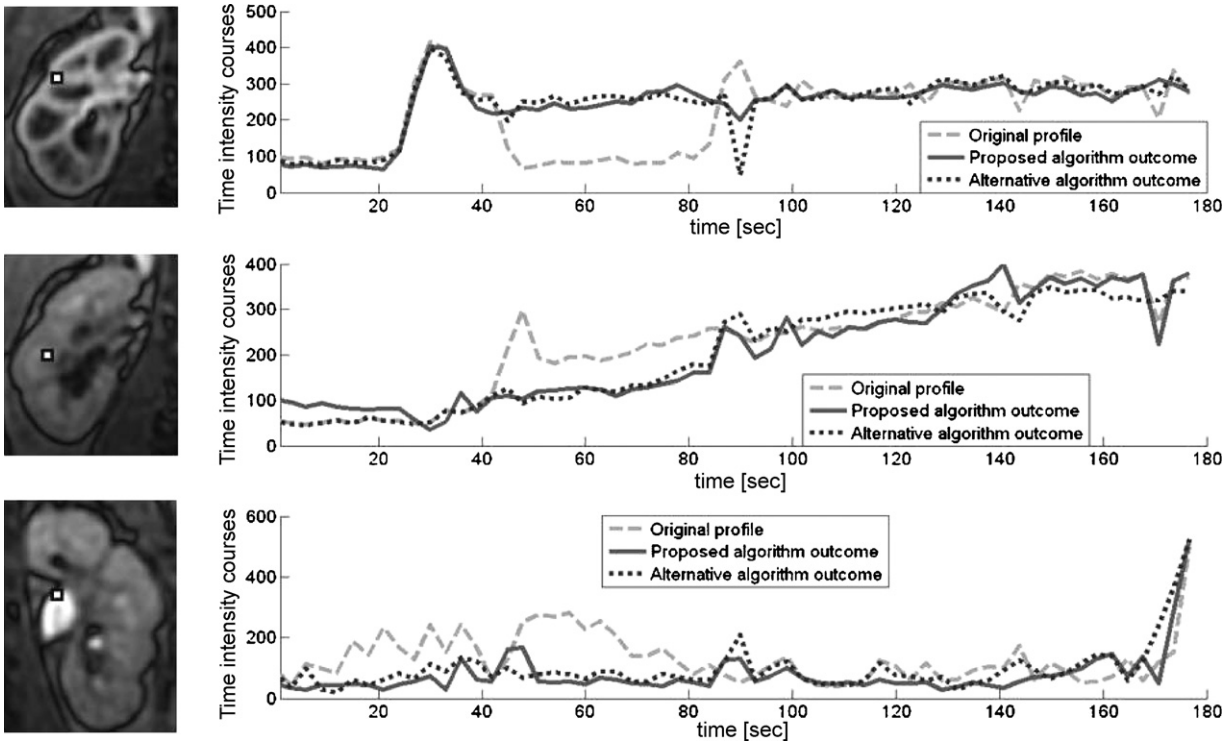

Fig. 3. Evaluation of the registration algorithm based on the comparison between the mean intensity time courses within a ROI before registration and after registration. ROI selection is depicted to the left of the time courses. The selected time frames are those where the kidney compartment is maximally enhanced: ~30 s, 100 s, and 170 s for the cortex, medulla, and pelvis, respectively. Data from exam 3.

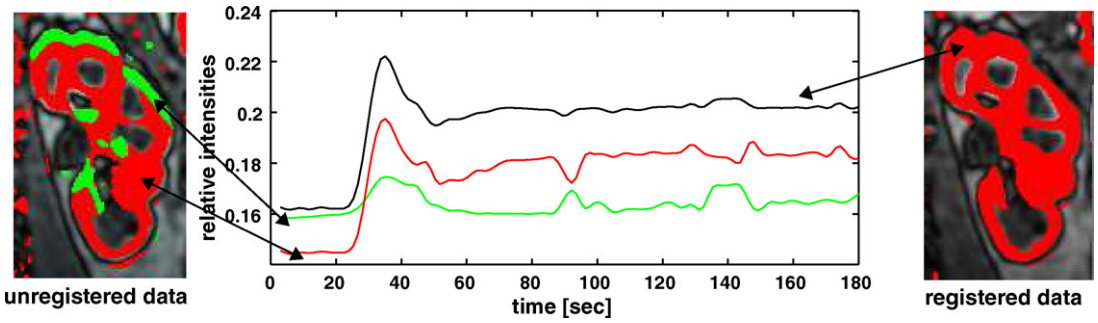

Fig. 4. Comparison of clustering results using registered and unregistered data, respectively. The left image depicts the renal cortex clusters obtained from unregistered data. The right image shows renal clusters after motion correction. In the middle the mean signal intensity time courses for the cortex regions are plotted. The black solid curve corresponds to the segmented (red) region on the right. The dashed and dotted curves represent time courses from red and green clusters (see arrows) in the left image, obtained without motion correction. Data from exam 3, slice 22/44. (For interpretation of the references to color in this figure legend, the reader is referred to the web version of the article.)

capture the comparison between the original images (dashed curves), those obtained from the application of the proposed registration algorithm (solid curves), and those obtained from the images registered with the alternative method (dotted curves). In these examples we have depicted the mean of the signal intensity values. Similar results were obtained for the remaining data sets.

In addition to depicting the mean signal intensity value of voxels included in the selected ROIs, we have also paid attention to the standard deviation of such a set of values. Table 2 shows the mean and median standard deviation obtained for data sets 1 and 3. Similar results are obtained for the other two data sets.

Analyzing the variances within the defined ROIs of registered and unregistered data by the *F*-test shows no significant differences ($p > 0.05$). However, looking at the individual time points, the variances and thus the standard deviations are significantly reduced compared to the unregistered cases. For example, within the ROI placed in the cortex of data set 3, in 50% of the time points a reduction by the alternative method could be obtained.

4.2. Impact of registration to clustering of voxel based time courses

In order to validate the complete processing of 3D DCE-MRI data, i.e. registration and clustering, we were interested in the impact of motion correction on the following clustering of the data. Therefore, we compared the clustering results of registered and unregistered data. The *k*-means clustering was initialized with the same parameters (cf. Section 3.3) as for the corresponding registered/unregistered pairs of each data set. Fig. 4 depicts such result for the left kidney of data set 3. Fig. 4 clearly shows that the clustering results in a different number of clusters (regions corresponding to the cortex) when unregistered and registered data are compared. In the unregistered case two regions representing the cortex (red and green, left image, Fig. 4) are found whereas in the motion-corrected case only one cortical region (red, right image, Fig. 4) is computed. Between the colored cluster regions, the corresponding derived time intensity curves are depicted.

4.3. Clustering of voxel-based time series

The evaluation of segmentation results is difficult, since in most cases, similar to the registration, no clear standards exist. As a qualitative evaluation we calculated the mean intensity time courses which have characteristic shapes for the segmented compartments and are used for further functional assessment of the kidney [14,10].

Figs. 5 and 6 show the clustering results of the separated kidneys of data sets 1 and 3 (1.5 T and 3 T scanner, respectively). For each obtained cluster the corresponding mean intensity time course was

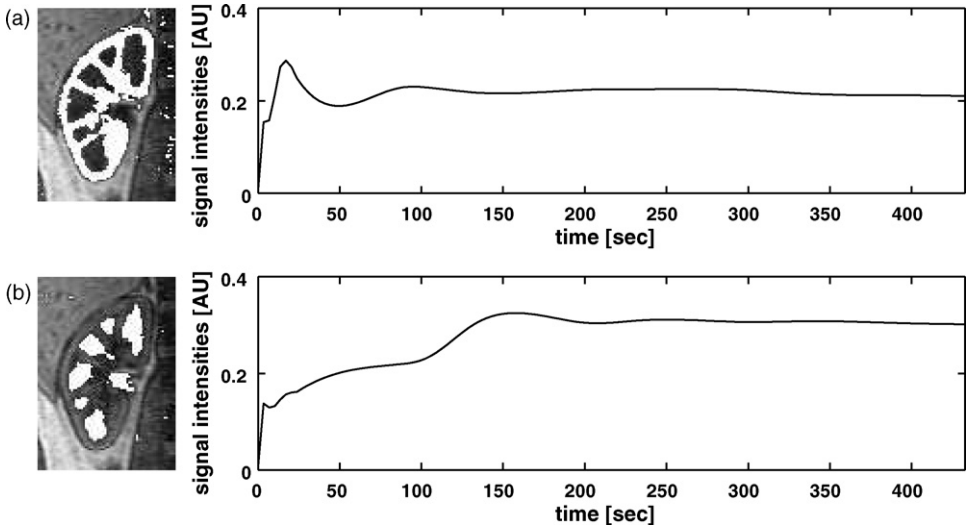

Fig. 5. Clustering results for exam 1, left kidney (slice 10/20, frame 2/20). The upper row (a) depicts the cluster (white segment) and corresponding mean signal intensity time course of the renal cortex. The lower row (b) depicts the cluster (white segment) and corresponding mean signal intensity time course of the renal collecting system. Notice that the time courses clearly identify the functional parts of the kidney (cortex and medulla/pelvis). Three other clusters (not shown) represent the background and partial volume effects.

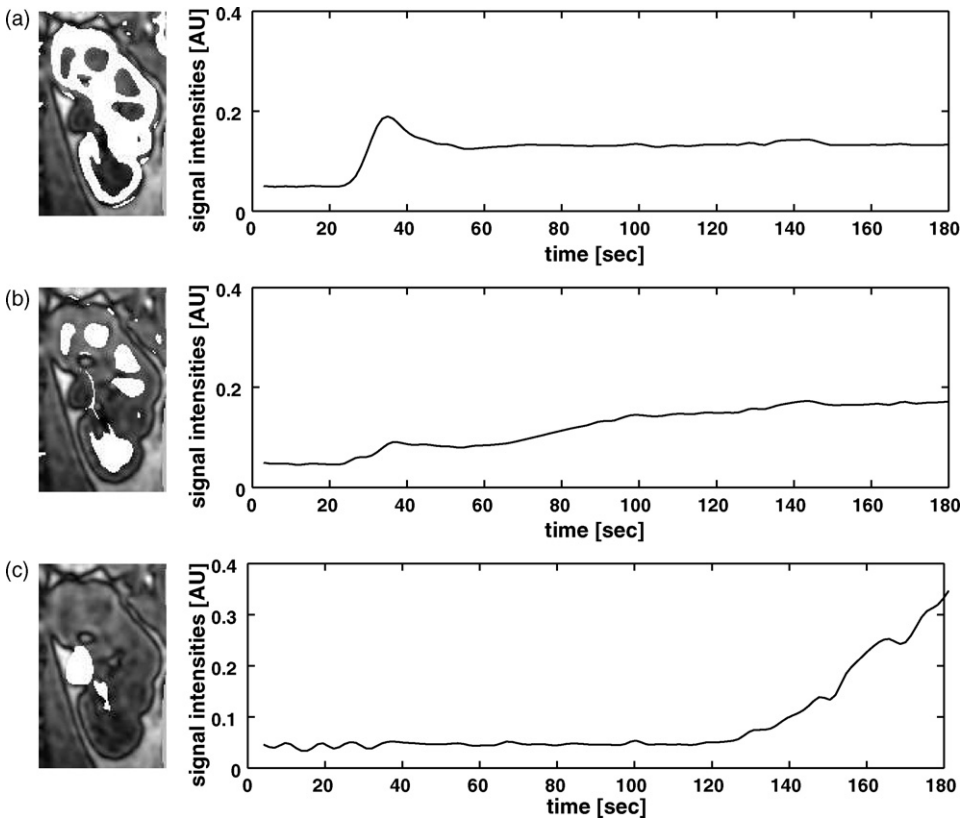

Fig. 6. Clustering results for exam 3, right kidney (slice 22/44, frame 2/60). The upper row (a) depicts the cluster (white segment) and corresponding mean signal intensity time course of the *renal cortex*. The middle row (b) depicts the cluster and corresponding mean signal intensity time course of the *renal medulla*. The lower row (c) depicts the cluster and corresponding mean signal intensity time course of the *renal pelvis*. *K*-means clustering was here initialized with $K = 7$. Four other clusters (not shown) represent the background and partial volume effects.

computed and plotted. In addition to these depicted time courses, a projection of the clustered region (bright pixels) onto the original image is given.

The clustering could detect the renal compartments (cortex, medulla) and in case of data set 3 also the pelvis (in data set 1 the pelvis and the medullary regions are merged but may be easily separated in a post-processing step). The other clusters collect background pixels as well as partial volume effects (data omitted). Similar results were retrieved for the other data sets.

In addition, manual delineations have been carried out by trained radiologists and compared to the regions derived from clustering.

Table 3 shows the results for the comparison based on the previously described Tanimoto (TN) overlap measure (cf. Section 3.3). For all four data sets high similarity could be obtained (average TN = 0.96). Standard deviations range between 1% and 6%.

The clustering results, i.e. the segmented kidney compartments could be directly serve as input for further processing or analysis. As an example, Fig. 7 depicts time-to-peak (TTP) maps derived automatically from the segmentation results.

Table 3
Evaluation of *k*-means based segmentation vs. manual segmentation.

Exam	TN	
	Mean	Std
1	0.95	0.06
2	0.96	0.01
3	0.96	0.03
4	0.97	0.01

The average Tanimoto measure (TN) and standard deviations (Std) over all slices and data sets are given. Slices for which no manual mask could be identified (outermost slices) were omitted from the evaluation.

5. Discussion

In this paper we have introduced a set of automated methods for the assessment of renal function from 3D DCE-MRI acquisitions, comprising multi-modal, non-rigid 3D image registration and *k*-means clustering that together enable the extraction of valid voxel time courses from recorded data. Up to now, the problem of kidney motion has generally been ignored when analyzing dynamic image data using model-free descriptive techniques or pharmacokinetic models [7–11]. However, registration should be an integral part of any analysis of such data since the motion, e.g. due to breathing, severely hampers the (voxelwise) time intensity curves which are used as input for pharmacokinetic modeling or semi-quantitative analyses.

The evaluation of image registration results is difficult since no clear standards exist for this kind of data [38]. Here, to assess the impact and performance of non-rigid image registration on voxel intensity time courses, we compared the results of two registration approaches developed by the authors. Inspecting Fig. 3, the registration methods could correct in most cases the time intensity curves compared to known shapes from literature [40]. Also, derived average standard deviations from carefully selected region of interest in the registered and unregistered data show a reduction in standard deviation for the proposed methods compared to the unregistered data, although the observed reduction is not significant. A rejection of the null hypothesis at 5% significance level was mostly not successful for data retrieved from images acquired at time points

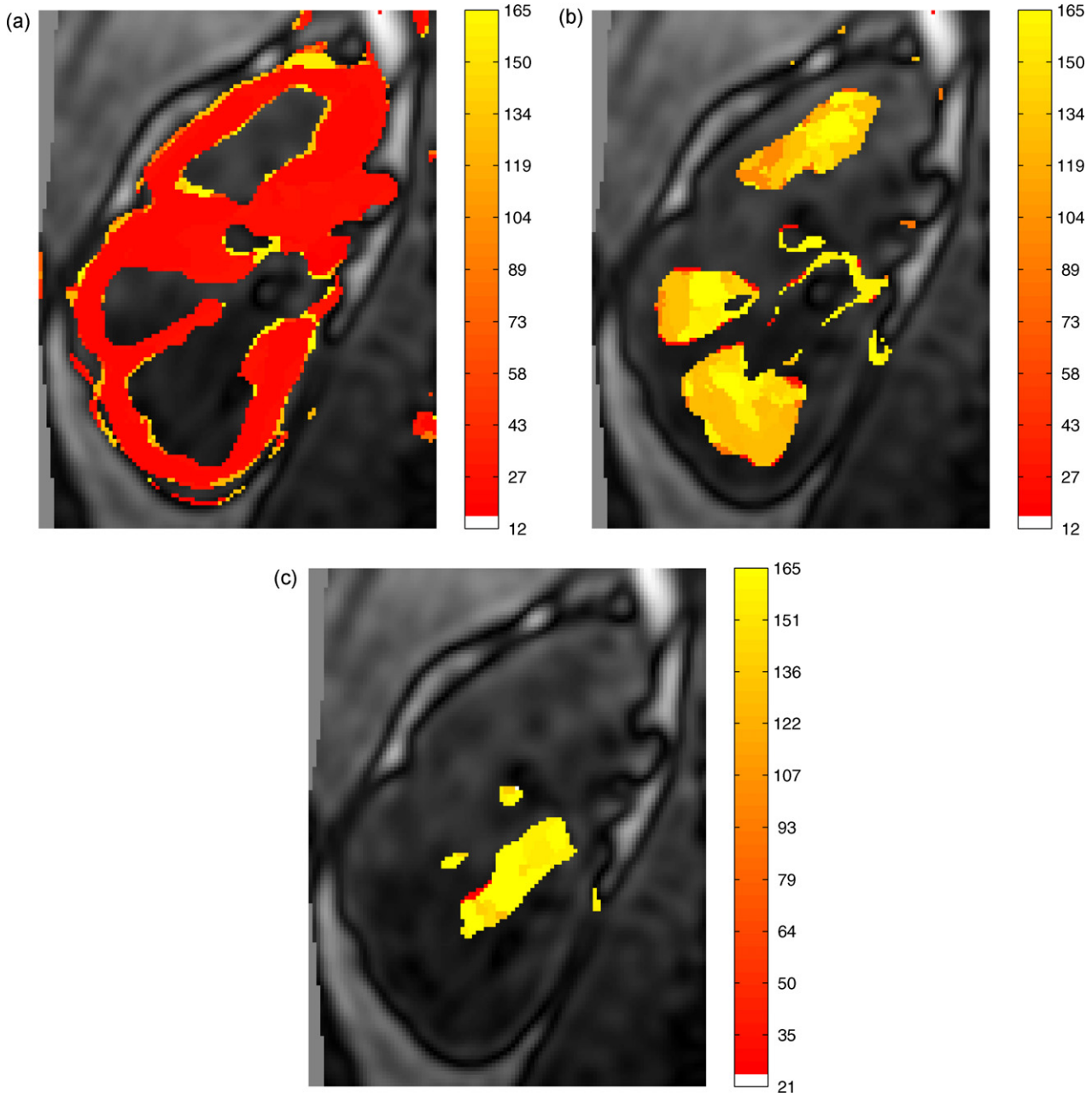

Fig. 7. Time-to-peak (TTP) parametric map of left kidney (exam 3) automatically calculated from the clustering results. Dark colors represent early arrival of contrast agent, light colors later arrival. The gray-scale bar to the right has values in seconds after contrast injection, where the contrast agent in this case was injected as a bolus after the fifth volume acquisition. Subfigure (a) depicts the cortex, (b) the medulla, and (c) the renal pelvis. (For interpretation of the references to color in this figure legend, the reader is referred to the web version of the article.)

of the first pass of the bolus (0–40 s). This is due to the acquisition scheme. Like others [11,10], we acquired these images during breath-hold, i.e. no or only few motion is present. Therefore, differences between registered and unregistered data might be low. On the other hand, this result also shows that the presented approaches do not distort the images if there is no or few motion. Furthermore, significant reduction in variances within ROIs correlates with time points surrounding breath-taking events during acquisition. This suggests that the developed registration algorithms could reduce the motion within DCE-MR image time series.

Since interpolation is implicitly required during the registration process, remaining differences between the two registration algorithms cannot be avoided when comparing the intensity courses (cf. Fig. 3). Also note that two very different registration algorithms are compared. Some differences are seen between results of each of the registration algorithms, especially for frames that were distorted due to extensive breathing motion. This is most noticeable for the cortex region in Fig. 3 at 90 s. However, in both cases, the time courses after registration are restored and characterize the tracer concentration profile expected for the corresponding renal compartments [12,40]. The time course computed from the same ROIs but without motion correction appears quite different and could compromise subsequent its further analyzes, either being model-free or model based.

Miscorrections only occur at time points where the subject takes breath (sharp peaks in the time courses). This seems to be difficult to handle for the registration approaches. To reduce such additional large breathing motion, probably a free breathing acquisition scheme might overcome this problem. In addition, some sort of respiratory gating could be applied [11] but temporal constraints

have to be taken care off when considering such approaches [41]. Furthermore, the absence of a gold standard certainly limits the explanatory power of the presented results. To overcome the lack of such a gold standard we are currently developing an in silico phantom of the kidney, allowing for superimposing – not only – motion [42]. With such a phantom, we hope to be able to evaluate the registration of DCE-MRI data in more detail.

Nevertheless, also without a gold standard the importance of the registration and therefore, the abilities of the presented approaches could be demonstrated. In Fig. 4, clustering results of registered and unregistered data are depicted. Imagine the case of a possible renal disease in a patient. On inspecting the left image in Fig. 4 the question arises of whether the black region represents a local defect in the kidney due to some kidney disease. In comparison to healthy cortex perfusion (black curve, Fig. 4), the corresponding mean intensity time course of the green region (green curve) seems to be degenerated. One might assume that renal disease was present. In this example, however, this is clearly misleading, since the data has been taken from a healthy volunteer. Healthy renal function – i.e. normal perfusion – is expected and no splitting of compartmental regions into separate clusters should occur. This is supported by the fact that the clustering seems to be sensitive to the data (cf. Table 3 and Fig. 6). Furthermore, when anatomical prior information is taken into account, all the regions obtained by clustering the unregistered data should have been associated with the renal cortex. The splitting of the cortex region in this example is clearly a result of motion artifacts present in the unregistered data. Data processing like our approach, including image registration, can thus be able to overcome these problems.

The conclusion is that proper registration will improve any subsequent analysis of DCE-MRI recordings. This is also confirmed by the recent work of Buonaccorsi et al. [13].

Furthermore, our results also show that clustering of time series enables the segmentation of the kidney into meaningful functional compartments, i.e. renal cortex, medulla, and pelvis. Comparing the segmentation results obtained by clustering, TN index values close to one could be achieved for most of the slices in the 3D volume (standard deviation ≤ 0.06 for all data sets). However, clustering becomes difficult towards the outermost slices, since the kidney is only partly visible, or not visible at all in these slices. Hence, manual delineation of the kidney also becomes difficult in these regions for the human observer. Therefore, these slices have been excluded from the evaluation.

Moreover, intensity time courses calculated from the *k*-means segmented regions were similar to corresponding time courses reported in the literature [12,40]: (i) early peak with steep up-slope corresponding to the first pass of the contrast agent through the vasculature of the cortex (cf. Fig. 6(a)), (ii) delayed and less distinct peak, representing filtered contrast agent in the tubular and collecting system of the medulla (cf. Fig. 6(b)), and (iii) very late ($\approx$120 s) enhancement of the pelvic region depicting the renal elimination of contrast agent in the urine (cf. Fig. 6(c)).

We conclude that *k*-means clustering is a suitable approach for time course analysis of renal perfusion studies when proper motion correction is performed as a preprocessing step. A benefit of this approach is that it is totally data-driven, requires no manual interaction (as compared to [16,17]), and therefore yields observer-independent results. In addition, it also allows for automated split function between left and right kidney.

Our approach so far only deals with the processing of observed signal time intensity courses. The voxel-by-voxel relationship between signal intensity evolution and the contrast agent concentration is actually non-linear and highly dependent on the pulse sequence and acquisition parameters being used, in addition to the intrinsic tissue T1 values [43]. In this paper, we have not considered any specific pharmacokinetic modeling framework; we have assumed that linear approximation is adequate for our illustrative purposes. Furthermore, more experiments on volunteers and patients should be carried out in order to optimize acquisition protocols and parameter settings for our image registration and segmentation algorithms.

In summary, we conclude that the results obtained so far are promising and show the potential of registration and automatic data analysis methods, especially if combined. We also demonstrated that registration, even without significant differences in variance within selected ROIS is important for subsequent processing of DCE-MRI data to obtain valid compartment segmentations and time courses, both important for the (automated) quantification of the physiology of kidney. By combining both of these methods, this approach provides a powerful tool for the assessment of renal function.

This work can form the basis for several further research directions. Firstly, parameter maps could be automatically derived from the clustered time courses, such as time-to-peak (TTP) maps for different segmented renal compartments. A graph, similar to Fig. 7, could be then used for the qualitative assessment of renal disease by clinicians and radiologists, or as an input for pharmacokinetic models. Secondly, clustering is only one approach to unsupervised, data-driven assessment of renal function. For example, independent component analysis has become a popular tool for fMRI data analysis of brain [44]. This method has been recently introduced by Zöllner et al. [45] to the study of renal DCE-MRI data, and could be compared to the *k*-means clustering methods.

In our future work we also plan to incorporate our methods into a pharmacokinetic modeling framework in order to estimate functional parameters, e.g., glomerular filtration rate. Accordingly, the methods presented in this paper could be seen as an important step towards an automatic and reliable approach to renal function analysis.

References

[1] Knoeppen BM, Stanton BA. Renal physiology. Mosby's physiology monograph. 4th ed. Elsevier; 2007.

[2] European Kidney Health Association. Factsheet: the kidney in health and disease. Last accessed on 9.8.2008; 2008. http://www.ekha.eu/D26CF/Info/Kidney_Fact_Sheets.aspx.

[3] Menon V, Gul A, Sarnak MJ. Cardiovascular risk factors in chronic kidney disease. Kidney Int 2005;68(4):1413–8.

[4] Myers GL, Miller WG, Coresh J, Fleming J, Greenberg N, Greene T, et al. Recommendations for improving serum creatinine measurement: a report from the laboratory working group of the national kidney disease education program. Clin Chem 2006;52(1):5–18.

[5] Prasad PV. Functional MRI of the kidney: tools for translational studies of pathophysiology of renal disease. Am J Physiol Renal Physiol 2006;290(5):F958–74.

[6] Michaely HJ, Schoenberg SO, Rieger JR, Reiser MF. MR angiography in patients with renal disease. Magn Reson Imag Clin N Am 2005;13(1):131–51, vi.

[7] Dujardin M, Sourbron S, Luypaert R, Verbeelen D, Stadnik T. Quantification of renal perfusion and function on a voxel-by-voxel basis: a feasibility study. Magn Reson Med 2005;54(4):841–9.

[8] Buckley DL, Shurrab AE, Cheung CM, Jones AP, Mamtora H, Kalra PA. Measurement of single kidney function using dynamic contrast-enhanced MRI: comparison of two models in human subjects. J Magn Reson Imag 2006;24(5):1117–23.

[9] Michoux N, Vallée J-P, Pechère-Bertschi A, Montet X, Buehler L, Beers BEV. Analysis of contrast-enhanced MR images to assess renal function. Magn Reson Mater Phys 2006;19(4):167–79.

[10] Lee VS, Rusinek H, Bokacheva L, Huang AJ, Oesingmann N, Chen Q. Renal function measurements from mr renography and a simplified multicompartmental model. Am J Physiol Renal Physiol 2007;292(5):F1548–59.

[11] Sourbron SP, Michaely HJ, Reiser MF, Schoenberg SO. MRI-measurement of perfusion and glomerular filtration in the human kidney with a separable compartment model. Invest Radiol 2008;43(1):40–8.

[12] Grenier N, Hauger O, Cimpean A, Pérot V. Update of renal imaging. Semin Nucl Med 2006;36(1):3–15.

[13] Buonaccorsi GA, Roberts C, Cheung S, Watson Y, O'Connor JPB, Davies K. Comparison of the performance of tracer kinetic model-driven registration for dynamic contrast enhanced mri using different models of contrast enhancement. Acad Radiol 2006;13(9):1112–23.

[14] Michaely HJ, Schoenberg SO, Oesingmann N, Ittrich C, Buhlig C, Friedrich D. Renal artery stenosis: functional assessment with dynamic MR perfusion measurements—feasibility study. Radiology 2006;238(2):586–96.
[15] de Priester JA, den Boer JA, Giele EL, Christiaans MH, Kessels A, Hasman A. MR renography: an algorithm for calculation and correction of cortical volume averaging in medullary renographs. J Magn Reson Imag 2000;12(3):453–9.
[16] Coulam CH, Bouley DM, Sommer FG. Measurement of renal volumes with contrast-enhanced MRI. J Magn Reson Imag 2002;15(2):174–9.
[17] Rusinek H, Boykov Y, Kaur M, Wong S, Bokacheva L, Sajous JB. Performance of an automated segmentation algorithm for 3D MR renography. Magn Reson Med 2007;57(6):1159–67.
[18] Zitova B, Flusser J. Image registration methods: a survey. Image Vision Comput 2003;21(4):977–1000.
[19] Maintz J, Viergever M. A survey of medical image registration. Med Image Anal 1998;2(1):1–36.
[20] Lee VS, Rusinek H, Noz ME, Lee P, Raghavan M, Kramer EL. Dynamic three-dimensional MR renography for the measurement of single kidney function: initial experience. Radiology 2003;227(1):289–94.
[21] Sun Y, Moura JMF, Ho C. Subpixel registration in renal perfusion MR image sequence. In: ISBI'04 IEEE international symposium on bioimaging, vol. 1. Arlington, VA: IEEE; 2004. p. 700–3.
[22] Song T, Lee VL, Rusinek H, Kaur M, Laine AF. Automatic 4-D registration in dynamic MR renography. In: IEEE-EMBS 2005. 27th Annual International Conference of the Engineering in Medicine and Biology Society, Vol. 3, IEEE, Shanghai, China, 2005, pp. 3067–3070.
[23] Rohlfing T, Maurer CR, O'Dell WG, Zhong J. Modeling liver motion and deformation during the respiratory cycle using intensity-based nonrigid registration of gated MR images. Med Phys 2004;31(3):427–32.
[24] Wismüller A, Meyer-Baese A, Lange O, Reiser M, Leinsinger G. Cluster analysis of dynamic cerebral contrast-enhanced perfusion MRI time-series. IEEE Trans Med Imag 2006;25(1):62–73.
[25] Ge Y, Law M, Johnson G, Herbert J, Babb JS, Mannon LJ. Dynamic susceptibility contrast perfusion MR imaging of multiple sclerosis lesions: characterizing hemodynamic impairment and inflammatory activity. AJNR Am J Neuroradiol 2005;26(6):1539–47.
[26] Baumgartner C, Gautsch K, Bhm C, Felber S. Functional cluster analysis of CT perfusion maps: a new tool for diagnosis of acute stroke? J Digit Imag 2005;18(3):219–26.
[27] Leinsinger G, Schlossbauer T, Scherr M, Lange O, Reiser M, Wismüller A. Cluster analysis of signal-intensity time course in dynamic breast MRI: does unsupervised vector quantization help to evaluate small mammographic lesions? Eur Radiol 2006;16(5):1138–46.
[28] Mouridsen K, Christensen S, Gyldensted L, Ostergaard L. Automatic selection of arterial input function using cluster analysis. Magn Reson Med 2006;55(3):524–31.
[29] MacQueen JB. Some methods for classification and analysis of multivariate observations. In: Proceedings of 5th Berkeley symposium on mathematical statistics and probability, vol. 1. Berkeley: University of California Press; 1967. p. 281–97.
[30] Coombs CH, Dawes RM, Tversky A. Mathematical psychology: an elementary introduction. Englewood Cliffs, NJ: Prentice-Hall; 1970.
[31] Yoo TS, editor. Insight into images, principles and practice for segmentation, registration, and image analysis. 1st ed. A K Peters Ltd.; 2004.
[32] Shanno DF. Conditioning of quasi-Newton methods for function minimization. Math Comput 1970;24:647–56.
[33] Sance R, Rogelj P, Ledesma-Carbayo MJ, Anderlik A, Zöllner F, Rørvik J. Motion correction in dynamic DCE-MRI studies for the evaluation of the renal function. Magn Reson Mater Phys 2006;19(Suppl. 7):106–7.
[34] Rogelj P, Kovacic S, Gee JC. Point similarity measures for non-rigid registration of multi-modal data. Comput Vision Image Understanding 2003;92(1):112–40.
[35] Rogelj P, Kovacic S. Symmetric image registration. Med Image Anal 2006;10(3):484–93.
[36] Bamberg G, Bauer F. Statistik, Oldenbourgs Lehr-und Handbücher der Wirtschafts-und Sozialwissenschaften. 2nd ed. Munich, Vienna: Oldenbourg; 1982.
[37] Qian G, Sural S, Gu Y, Pramanik S. Similarity between euclidean and cosine angle distance for nearest neighbor queries. In: SAC'04: proceedings of the 2004 ACM symposium on applied computing. New York, NY, USA: ACM; 2004. p. 1232–7.
[38] Crum W, Camara O, Hill D. Generalized overlap measures for evaluation and validation in medical image analysis. IEEE Trans Med Imag 2006;25(11):1451–61.
[39] Martin-Fernandez M, Bouix S, Ungar L, McCarley RW, Shenton ME. Two methods for validating brain tissue classifiers. In: Duncan J, Gerig G, editors. 8th international conference on medical image computing and computer-assisted intervention, no. 3749 in lecture notes in computer science. Berlin, Heidelberg, Palm Springs, CA, USA: Springer–Verlag; 2005. p. 515–22.
[40] Michaely HJ, Herrmann KA, Nael K, Oesingmann N, Reiser MF, Schoenberg SO. Functional renal imaging: nonvascular renal disease. Abdom Imag 2007;32(1):1–16.
[41] Michaely HJ, Sourbron SP, Buettner C, Lodemann K-P, Reiser MF, Schoenberg SO. Temporal constraints in renal perfusion imaging with a 2-compartment model. Invest Radiol 2008;43(2):120–8.
[42] Anderlik A, Zöllner FG, Rørvik J, Lundervold A, Munthe-Kaas A. Functional kidney imaging in silico—a framework for studying motion correction and pharmacokinetics. Magn Reson Mater Phys Biol Med 2008;21(Suppl. 1):447–8.
[43] Armitage P, Behrenbruch C, Brady M, Moore N. Extracting and visualizing physiological parameters using dynamic contrast-enhanced magnetic resonance imaging of the breast. Med Image Anal 2005;9(4):315–29.
[44] Calhoun VD, Adali T. Unmixing fMRI with independent component analysis. IEEE Eng Med Biol Mag 2006;25(2):79–90.
[45] Zöllner FG, Lundervold A, Kocinski M, Rørvik J. Assessment of renal function from 3D dynamic contrast enhanced MR images using independent component analysis. In: Meinzer H-P, Handels H, Horsch A, Deserno T, Tolxdorff T, editors. Bildverarbeitung für die Medizin 2007—Algorithmen, Systeme, Anwendungen, Informatik Aktuell. Springer; 2007. p. 238–41.

Frank G. Zöllner received the diploma and a PhD degree (Dr.-Ing.) in computer science from the University of Bielefeld, Germany, in 2001 and 2004, respectively. He joined the Applied Computer Science group in 2001 and worked towards his PhD within the bioinformatics graduate program until 2004. From 2004 until 2006 he worked as a post-doctoral researcher in the BMBF project ALPIC. From February to May 2006 he was a guest researcher at the Computational Biology Unit, Bergen Center for Computational Sciences, University of Bergen. From May 2006 until December 2007 he was a researcher at the Section of Radiology, Institute for Surgical Sciences, Haukeland University Hospital and the Neuroinformatics and Image Analysis Group, Department of Biomedicine at the University of Bergen, Norway. Currently, he holds a 10% research position at the Section of Radiology, Institute for Surgical Sciences, Haukeland University Hospital. In 2008, Dr. Zöllner joined the Chair of Computer Assisted Clinical Medicine as a post-doctoral researcher. His research interests lie in the fields of pattern recognition, image processing as well as bioinformatics. In particular, he is interested in applying computational methods from pattern recognition, image analysis, or bioinformatics to the fields of molecular imaging and medical image analysis. Currently, he works on magnetic resonance imaging (MRI) of the human kidney for diagnostics of renal disease. Dr. Zöllner is a member of the IEEE Computer Society and the European Society for Magnetic Resonance in Medicine and Biology (ESMRMB).

Rosario Sance received a MEng degree in 2005 from Univ Politécnica de Madrid (UPM), with a master thesis on "MRI registration for the evaluation of the renal function". Currently she is working for a PhD thesis in the Biomedical Image Technology group (BIT), included in the Electronic Eng. Dept. (UPM). In the framework of the project COSTB21 (Physiological Modelling of MR Image Formation), she has been working in the analysis of kidney function in collaboration with University of Bergen (Norway). Her research interests are medical image analysis, mainly image registration and dynamic image analysis.

Peter Rogelj received a PhD degree in electrical engineering from the University of Ljubljana (ULJ), Slovenia, in 2003. He joined the Machine Vision Group at ULJ in 1998. During his study towards a master's degree (2001) and the PhD degree, he also worked as a guest researcher at Czech Technical University, Prague, CZ, and University of Pennsylvania, Philadelphia, USA. Later he conducted several research projects in ULJ and in industry. His main research interest is image processing, with a special focus on multi-modality and non-rigid medical image registration.

María J. Ledesma-Carbayo graduated in telecommunication engineering in 1998, with a master thesis on medical image analysis. Previously, in 1997/1998, she followed the ERASMUS European Course on Biomedical Engineering and Medical Physics in Univ. Patras (Greece). She is now associate professor in the Electronics Eng. Dept. (Universidad Politécnica de Madrid), and she has obtained her PhD degree in biomedical imaging several years ago. In 1999, she has visited the Medical Vision Lab. at Oxford Univ. during three months and in 2000 and 2001, she has collaborated with École Polytechnique Fédéral in Lausanne (Switzerland). Recently she has spent six months on the Cardiac Energetics Lab. at the National Institutes of Health (USA). Her main research areas of interest are medical image analysis and processing, especially those topics dealing with registration, cardiac imaging and motion estimation and compensation. Her research in medical imaging processing has been published in journals and conferences (more than 50). She has a lot of experience participating in research projects, from the Spanish Finantial Offices, International Agencies and International Companies. Member of IEEE.

Jarle Rørvik has a position as associate professor in radiology at the University of Bergen and physician at the Department of Radiology at Haukeland University Hospital, Bergen, Norway.

In 1998 he finished his thesis on use of imaging for staging organ-confined prostate cancer prior to radical treatment. Later he has continued his research on prostate cancer both for detection and staging. Currently, he and his research team perform studies on use of MRI with contrast and MR spectroscopy for both detection and staging of prostate cancer.

Further, he has together with Arvid Lundervold established a research-group working with MRI for kidney imaging including both morphologic and functional exams. He has been supervisor for two PhD-students (doctores medicalis) and several masterstudents with a wide spectrum of research topics.

He is in charge of the education of medical students in radiology and has received several prizes for the quality in the teaching. A special interest has been developement and use of digital teaching material for the internet.

Andrés Santos has a PhD and a MEng from Universidad Politécnica Madrid (UPM). He has a position as professor in the Electronic Engineering Dept. (UPM), where he is the Director of the Biomedical Image Technology group since it was founded in

2000. During 1987–1988 he was International Research Fellow at SRI International (Menlo Park, California). He has been co-director of a master course in biomedical enginering and since 1995 he is also professor in the European Course on Biomedical Engineering (Univ. Patras, Greece).

His research interests are related to biomedical image acquisition and analysis. Coordinator of several national and international projects on biomedical imaging and author or co-author of more than 150 international publications. Member of SPIE, IEEE and ESEM.

Arvid Lundervold has a BSc in mathematics and got his medical training (MD) from University of Oslo. He has a PhD on "Multispectral analysis, classification and quantification in medical magnetic resonance imaging" from University of Bergen in 1995. He has been a research scientist at the Norwegian Computing Center in Oslo, working on image analysis and pattern recognition, and later associate professor at Department of Physiology, University of Bergen. From September 2005 he has been professor in medical information technology at Department of Biomedicine, University of Bergen and is head of the Neuroinformatics and Image Analysis Laboratory. He is also member of the Molecular Imaging Center, UoB, the Bergen fMRI group, and the interdisciplinary Bergen Image Processing group, located at the Department of Mathematics. He his participating in several national and international projects, and member of IEEE Computer Society, ISMRM, MAA and the Norwegian Medical Association.